Progress In Electromagnetics Research M, Vol. 62, 143–151, 2017

Compact Dual-Band Inverted-F Filtering Antenna Using Dual-Mode Resonators

Tianming Yang*, Deqiang Yang, Kai Sun, and Jianzhong Hu

Abstract—A compact dual-band inverted-F filtering antenna with good band-edge selectivity for modern wireless communication systems is presented in this paper. A novel dual-band filter based on open-loop dual-mode resonator loading a T-shaped stub and an inverted-F antenna (IFA) also with a T-shaped open stub are integrated together. The higher band is controllable easily by adjusting the dimension of the T-shaped stub, leaving the lower band unaffected. To minimize the dimension of the filtering antenna, the last stage of the filter is folded. A flat gain response is obtained with steep skirts at both band edges. Simulated and measured results show that the integration makes the proposed antenna operate at 2.4/3.7 GHz with compact size, good band-edge selectivity, and controllable higher band compared with the traditional IFA.

1. INTRODUCTION

The modern wireless communication systems have been experiencing a rapid development in the last few decades. As the most important part in the entire wireless communication systems, the RF front-ends need to have excellent features such as multiband, controllable band, compact size, low insertion loss and good band-edge selectivity. Compared with other components, the filters and antennas, which are designed individually and then connected by the transmission line conventionally, are larger and cause more insertion loss. Thus, there will be great benefits if the antennas and filters are integrated into one compact module to provide both the desired filtering and radiating performances. First, it makes the RF front-ends more compact due to the co-design. Second, the insertion loss will be reduced obviously which is caused by the connection between the filters and antennas. Third, it can avoid the electromagnetic interference (EMI) problem caused by other systems. Up to now, the main types of filtering antennas can be summarized as: (i) planar ultra-wideband (UWB) antennas with band-notched characteristic [1–3]. (ii) horn antennas with integrated notch filter [4]. (iii) planar monopole filtering antennas [5, 6].

Several efforts have been made to replace the last stage of the filter with a radiator [7–9] without the need of extra circuit area. These works integrate the antennas and filters successfully which can realize good impedance matching and steep band-edge selectivity. Nevertheless, these designs can only realize a single band which is not suitable for practical applications when multi-band operation has become a necessity. This situation is caused by the need of a quarter-wavelength coupled line which is treated as the admittance inverter. In [10], a multiband filter and monopole antenna are cascaded directly to realize a tri-band filtering antenna without a fully integrated process while its size is large. A compact dual-band filtering patch antenna using step impedance resonators with harmonic suppression and controllable bandwidth is reported in [11]. However, the need of matching section decreases the radiation efficiency, and the use of 3-layer PCB creates added complexity. Its gain is low at the same

Received 20 September 2017, Accepted 10 November 2017, Scheduled 17 November 2017
* Corresponding author: Tianming Yang (tmy_uestc@163.com).
The authors are with the School of Electronic Engineering, University of Electronic Science and Technology of China, Chengdu, Sichuan, China.

time. The peak gains at 2.45 and 5.8 GHz are −1.8 and 1.1 dBi, respectively. Up to date, it is quite a challenging task to design a multiband filtering antenna.

The mainstream design method for filtering antennas is still replacing the last stage of the filter with a radiator. The success of these designs is that the last stage of filter is replaced by a quarter-wavelength coupled line which can reduce the circuit size obviously while providing both the desired filtering and radiating performances. However, only single band operation can be realized. So, the traditional method should be improved to be suitable for dual-band applications while keeping antennas compact. Considering the essence that these designs also need cascade the filter with antenna directly using a quarter-wavelength coupled line, the design in this paper applies two stub-loaded resonators (SLRs) to realize dual-band performance and good band-edge selectivity while the filtering antenna remains miniaturized by modifying the last stage of the filter. The integration of the dual-band filter and IFA on the same layer of the substrate not only enables the proposed antenna to operate at 2.4/3.6 GHz, which can be applied to the 2.4G WLAN (2.412–2.472 GHz) and 3.7G LTE Band 43 (3.6–3.8 GHz) communication systems, but also obtains steep band selectivity at both band edges. Above all, the higher band is controllable easily by adjusting the dimension of the T-shaped stub, leaving the lower band unaffected, which increases the flexibility of the design.

All the designs in this paper are based on the substrate Rogers RO4350B. Its relative permittivity is 3.48, loss tangent 0.004, thickness 0.762 mm and thickness of electrodeposited copper 35 μm. And the simulated results are calculated by the finite element method (FEM) based on ANSOFT High Frequency Structure Simulation (HFSS v. 15.0).

2. DESIGN OF SLRS-BASED DUAL BAND FILTER

Figure 1(a) shows the proposed T-shaped stub-loaded open-loop resonator which contains one conventional microstrip half-wavelength resonator and one T-shaped open stub, where θ_1, θ_2, θ_3 are the electrical lengths of the microstrip, respectively, and Y_1, Y_2, Y_3 represent their characteristic admittances. The lines T-T' represent its symmetrical planes. Figure 1(b), Figure 1(c) show the odd-mode and even-mode equivalent circuits of the resonator, respectively. For odd-mode excitation, replacing the symmetrical planes T-T' by an electric wall means that there is a voltage null along it. This leads

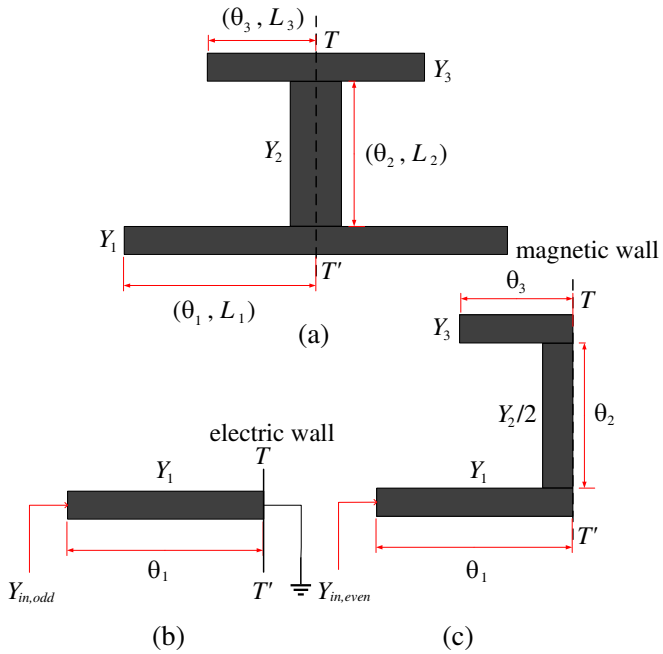

Figure 1. (a) Structure of the T shape stub-loaded open-loop resonator, (b) odd-mode equivalent circuit, (c) even-mode equivalent circuit.

to short circuit. For even-mode excitation, replacing the symmetrical planes T-T' by a magnetic wall means that there is no current flowing through it, and this leads to open circuit.

According to the transmission line theory [12], the relation between the input admittance Y_{in} and load admittance Y_l at any position of the transmission line is

$$Y_{in} = \frac{1}{Z_{in}} = \frac{1}{Z_0}\frac{\frac{1}{Z_l} + j\frac{1}{Z_0}\tan\theta}{\frac{1}{Z_0} + j\frac{1}{Z_l}\tan\theta} = Y_0\frac{Y_l + jY_0\tan\theta}{Y_0 + jY_l\tan\theta} \tag{1}$$

where θ is the electrical length of the transmission line, and Y_0 represents its characteristic admittance. Z_l and Z_0 are its load impedance and characteristic impedance, respectively.

The load impedance Y_l of the odd-mode equivalent circuit is ∞, and the characteristic admittance Y_0 of the microstrip for it is equal to Y_1. Therefore, the input admittance for odd-mode can be expressed as:

$$Y_{in,odd} = \frac{Y_1}{j\tan\theta_1} \tag{2}$$

The resonance condition is that the input admittance must be equal to zero, which means that the following condition must be met.

$$\theta_1 = n\pi/2 \tag{3}$$

Thus, the odd-mode resonant frequencies can be expressed as:

$$f_{odd} = \frac{nc}{4L_1\sqrt{\varepsilon_{eff}}}, \quad n = 1, 2, 3, \ldots \tag{4}$$

Similarly, for the special case of $Y_1 = Y_3 = Y_2/2$, the input admittance and resonant frequencies for even-mode can be expressed as:

$$Y_{in,even} = jY_1\tan(\theta_1 + \theta_3 + \theta_3) \tag{5}$$

$$f_{even} = \frac{nc}{2(L_1 + L_2 + L_3)\sqrt{\varepsilon_{eff}}}, \quad n = 1, 2, 3, \ldots \tag{6}$$

where L_1, L_2, L_3 are the physical lengths of the microstrip, respectively. ε_{eff} is the effective permittivity of the dielectric substrate.

According to Equations (4) and (6), the odd-mode resonant frequencies have nothing to do with the values of L_2, L_3. Therefore, adjusting the length of the T-shaped stub can change the even resonant frequencies, and the odd-mode resonant frequencies remain unchanged, which means that one can change the higher band easily by adjusting the dimension of the T-shaped stub while leaving the lower band unaffected.

Based on the resonators loading the T-shaped stub, a dual-band bandpass filter with a 0° feed structure [13] is designed. This feed structure can create three extra transmission zeros in the stopband at 1.9, 2.9, 4.1 GHz which means that good band-edge selectivity can be realized. The filter's design layout and equivalent circuit are depicted in Figure 2(a) and Figure 2(b), respectively. Electric coupling between the two resonators is realized by this configuration which was studied in [14–16] previously. Replacing the symmetrical plane O-O' by an electric wall, the odd-mode resonance frequencies of the resultant circuit can be deduced as:

$$f^o_{L,H} = 1\Big/\left\{2\pi\left[L_{L,H}\left(C_{L,H} + C^m_{L,H}\right)\right]^{1/2}\right\} \tag{7}$$

Similarly, when it is replaced by a magnetic wall, the resultant circuit has even-mode resonance frequencies as:

$$f^e_{L,H} = 1\Big/\left\{2\pi\left[L_{L,H}\left(C_{L,H} - C^m_{L,H}\right)\right]^{1/2}\right\} \tag{8}$$

where $L_{L,H}$ and $C_{L,H}$ are the self inductance and capacitance of the uncoupled SLRs, respectively. $C^m_{L,H}$ is the coupling capacitance between the two SLRs. The subscripts L, H represent the lower and higher bands of the SLRs, respectively.

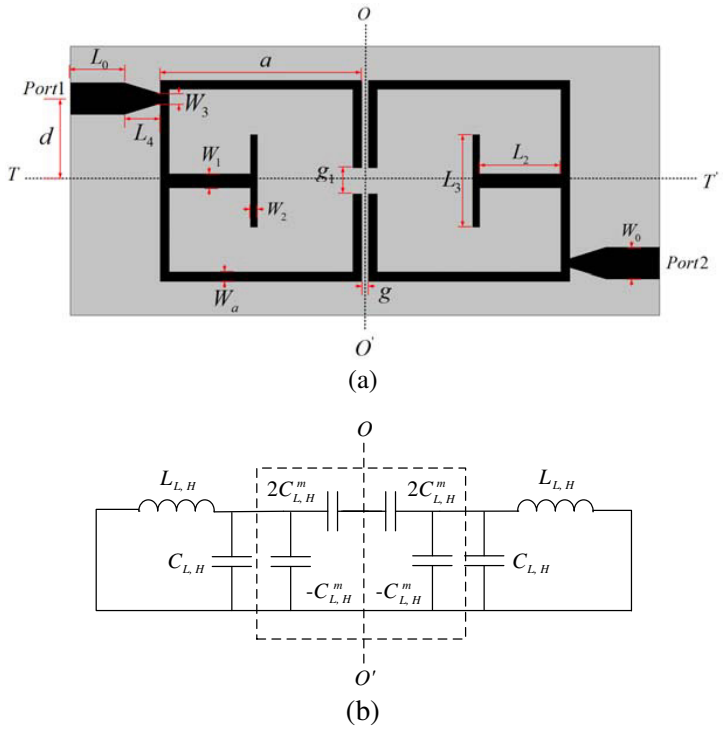

Figure 2. Dual band filter based on two electric coupled dual-mode resonators. (a) Design layout, (b) equivalent circuit.

Firstly, the T-shape stub-loaded open-loop resonator has two basic resonant frequencies $f_{odd}(f_L)$, $f_{even}(f_H)$. Then, the electric coupling between the two resonators produces two resonance frequencies (f^o, f^e) in the lower or higher bands, respectively. Thus, four resonance frequencies ($f^o_L, f^e_L, f^o_H, f^e_H$) are obtained, and the lower passband frequencies are mainly determined by the dimensions of the open loop resonator while the higher passband frequencies can be controlled easily by adjusting the dimensions of the T-shaped stub, and the passband bandwidths of this filter depend on the gap g and distance d. Thus, the increase of the values of L_2 and L_3 will decrease the higher frequencies. As shown in Figure 3, the increase of the value of L_2 decreases the higher frequencies. The values of the design parameters for the proposed filter are chosen as follows: $a = 11.2\,\text{mm}$, $W_a = 0.5\,\text{mm}$, $W_0 = 1.75\,\text{mm}$, $L_0 = 3\,\text{mm}$, $W_1 = 0.8\,\text{mm}$, $L_4 = 2\,\text{mm}$, $W_2 = 0.4\,\text{mm}$, $L_2 = 3.8\,\text{mm}$, $W_3 = 0.5\,\text{mm}$, $L_3 = 5.4\,\text{mm}$, $d = 4.4\,\text{mm}$, $g = 0.35\,\text{mm}$, $g_1 = 1.5\,\text{mm}$.

To miniaturize the dimension of the filter, the last stage resonator of the filter is folded as shown in Figure 4. Its resonant frequency must be tuned to be close to the first SLR's, but not necessarily equal. Thus, two symmetrical strips are added to make the modified resonator's resonant frequency nearly equal to the first SLR's. Besides, the coupling efficiency between the two resonators of the miniaturized filter remains almost unaffected because the coupling between the two strips and the first SLR is very weak when the space between them is large enough. Figure 5 gives the simulated S-parameters of the modified filter. Although only two resonance frequencies (f_L, f_H) are obtained because the modification makes the coupling between the two SLRs stronger, this has little influence on the bandwidth of the passbands.

3. DESIGN OF COMPACT DUAL BAND FILTERING ANTENNA

Inspired by the characteristic of the proposed filter that the higher band is controllable easily, a compact IFA also loading a T-shaped stub is designed. The top and bottom views of the proposed compact IFA are shown in Figure 6. Figure 7 gives the simulated surface current vector of the IFA at 2.45 and 3.65 GHz. The current intensity on the T-shaped stub is very weak at 2.45 GHz, but it is strong at

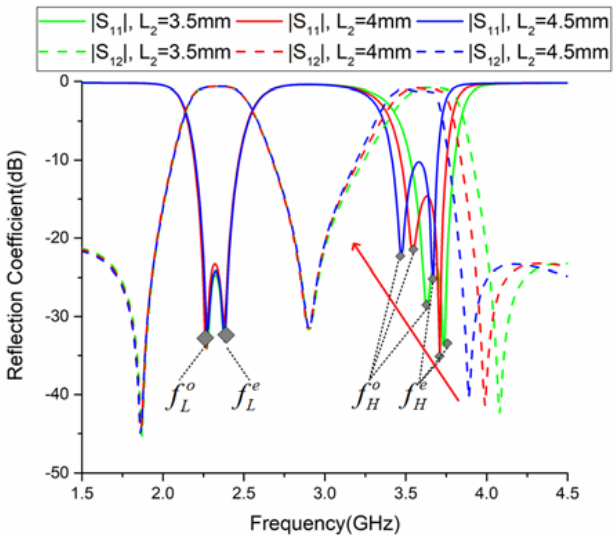

Figure 3. Simulated S-parameters of the electric coupled filter when the length of L_2 is varied from 4.5 to 3.5 mm.

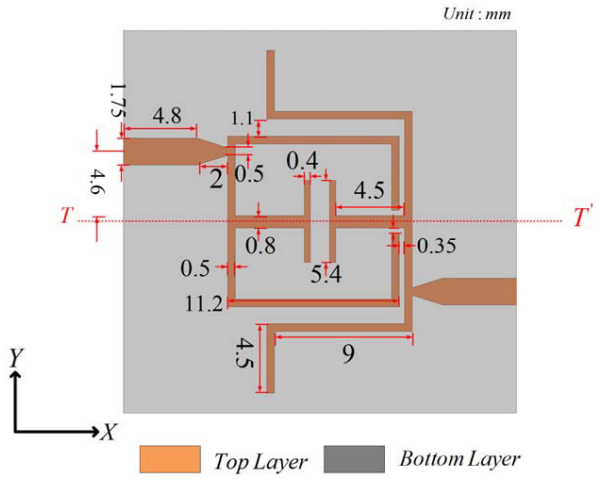

Figure 4. The design layout of the modified filter.

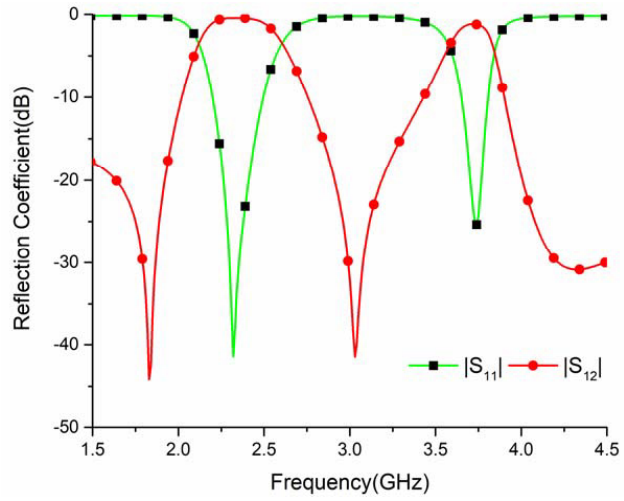

Figure 5. Simulated S-parameters of the modified filter.

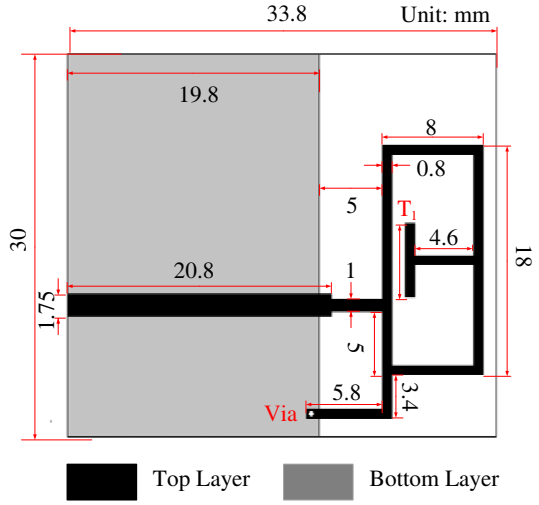

Figure 6. The proposed IFA loading T shape stub.

3.65 GHz. Thus, the increase of the length of T_1 has little impact on the lower band but decreases the central frequency of the higher band. As shown in Figure 8, the central frequency of the higher band decreases when the length of T_1 varies from 4.0–6.0 mm while the lower band is unaffected.

Inspired by the mainstream design method for filtering antenna in [7–9] which replaces the last stage of the filter with a quarter-wavelength coupled line and a radiator, the last stage of the filter in Figure 2 is modified. This modification makes the second SLR act as a dual-band admittance inverter. And its resonant frequencies must be tuned to be close to the first SLR's, but not necessarily equal. Due to the modification, the dimension of the filter is reduced obviously while its performances remain unaffected. Ultimately, a compact filtering antenna with a modified second-order dual-band filter and an IFA is integrated and optimized together. The whole size of the filtering antenna is $33.8 \times 30 \times 0.762\,\text{mm}^3$. The configuration of the filtering antenna is shown in Figure 9(a). A prototype as shown in Figure 9(b) is fabricated and measured. The scattering parameters of the antenna are measured by a vector network

analyzer (Agilent N5235A). And its radiation characteristics are measured in a $25\times15\times15\,\mathrm{m}^3$ anechoic microwave chamber at the University of Electronic Science and Technology of China.

The simulated reflection coefficient and peak gain in the $XOY(E)$-planes of the filtering antenna comparing with the IFA are shown in Figure 10. It is obvious that a flat gain response is obtained within the passband with steep skirts at both band edges compared with the IFA. The simulated impedance

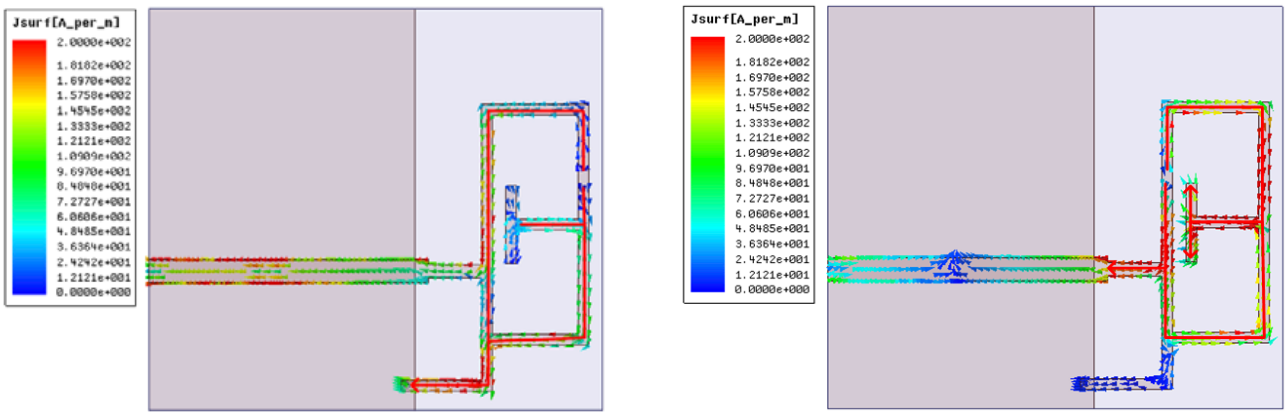

(a) (b)

Figure 7. Simulated surface current vector at different frequencies, (a) 2.45 GHz, (b) 3.65 GHz.

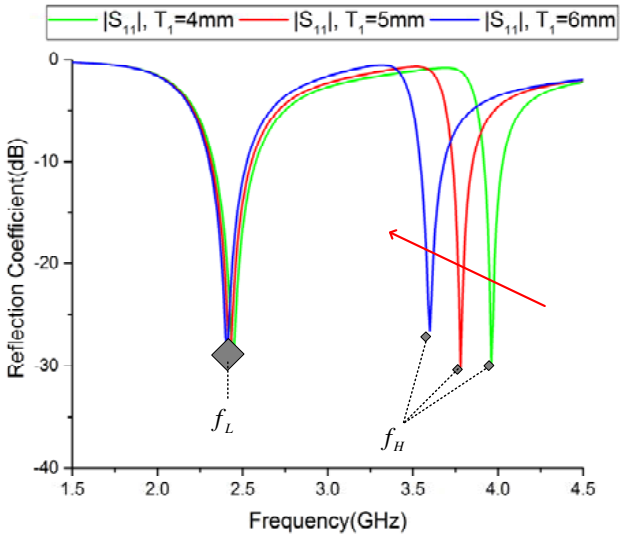

Figure 8. Simulated reflection coefficient of the IFA when the length of T_1 is varied from 4 to 6 mm.

Table 1. Summary of the performance of the filtering antennas.

Filtering antenna	Size	Frequency band	Operating frequencies (GHz)	Peak gain (dBi)
[5]	$0.41\lambda_g \times 0.6\lambda_g$	Single-band	2.45	2.41
[10]	$0.38\lambda_g \times 0.77\lambda_g$	Tri-band	2.4/5.2/6.5	2.1; 4.1; 4.6
[11]	$0.68\lambda_g \times 0.96\lambda_g$	Dual-band	2.4/5.8	-1.8; 1.1
Proposed	$0.43\lambda_g \times 0.39\lambda_g$	Dual-band	2.4/3.6	1.38; 1.58

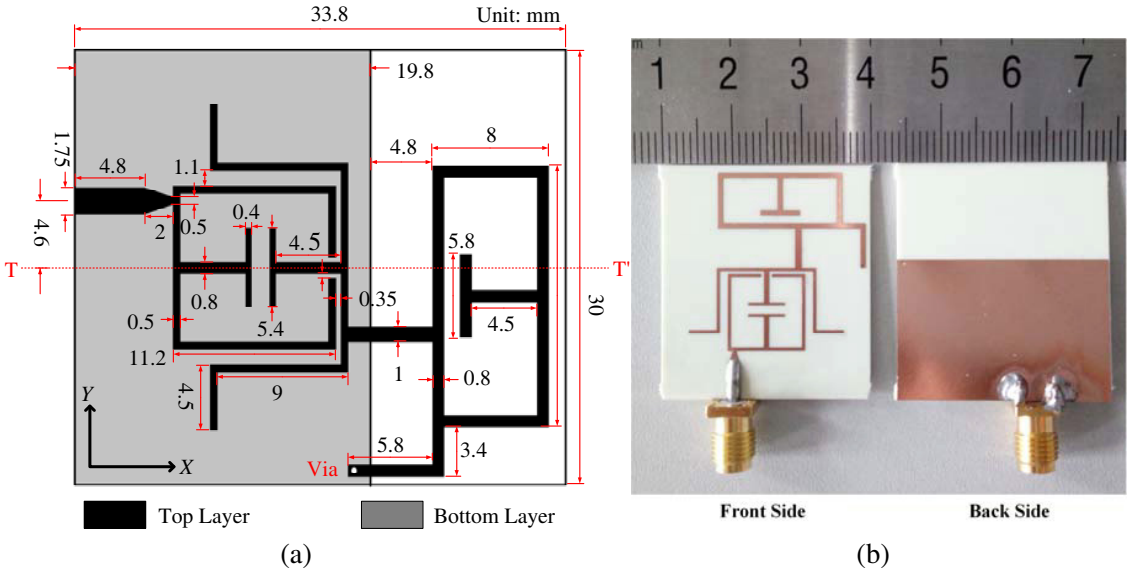

Figure 9. The proposed compact dual-band inverted-F filtering antenna. (a) Design layout, (b) photography of the proposed antenna.

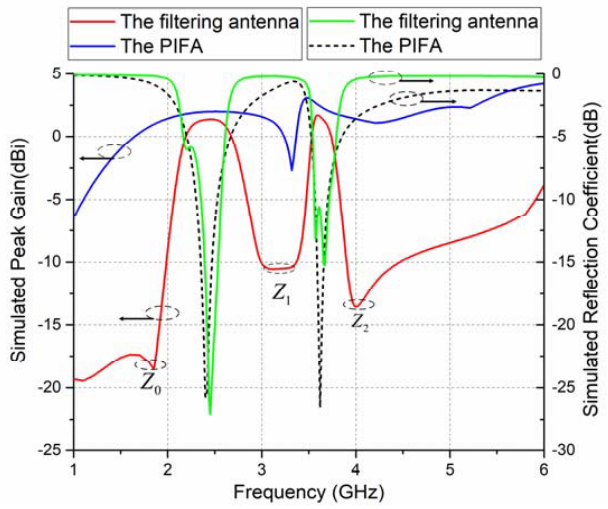

Figure 10. Simulated reflection coefficient and peak gain of the filtering antenna comparing with the IFA.

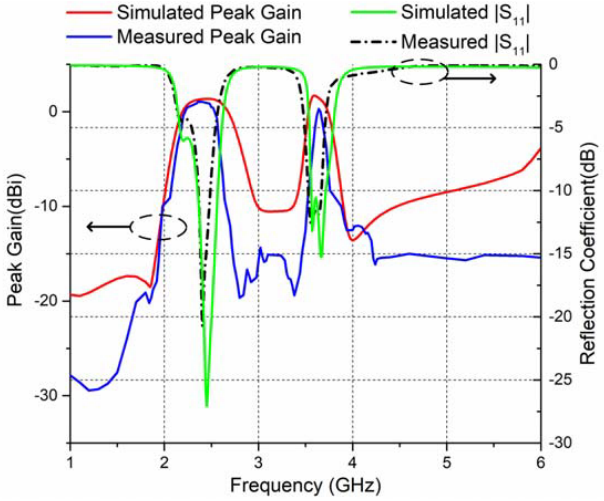

Figure 11. The simulated and measured reflection coefficient and peak gain of the filtering antenna.

bandwidths of the filtering antenna, with $|S_{11}| < -10$ dB, are from 2.35 to 2.57 GHz and from 3.56 to 3.81 GHz (8.9% and 4.4% fractional impedance bandwidth, respectively). The simulated peak gains at 2.46 and 3.64 GHz central frequencies of the passbands are 1.38 and 1.58 dBi, respectively. Besides, three radiation zeros in the stopband at 1.85, 3.2 and 4.0 GHz are obtained which means that good band-edge selectivity is realized.

Figure 11 shows the simulated and measured reflection coefficients and peak gains in the $XOY(E)$-planes of the filtering antenna. Very good agreement is obtained between the simulated and measured results with only bandwidth of the passband slightly narrower than predicted one. Both results confirm that the filtering antenna achieves flat gain response in the passband and good band-selectivity. The simulated and experimental radiation patterns at 2.46 and 3.64 GHz in XOY- and YOZ-planes are also given in Figure 12.

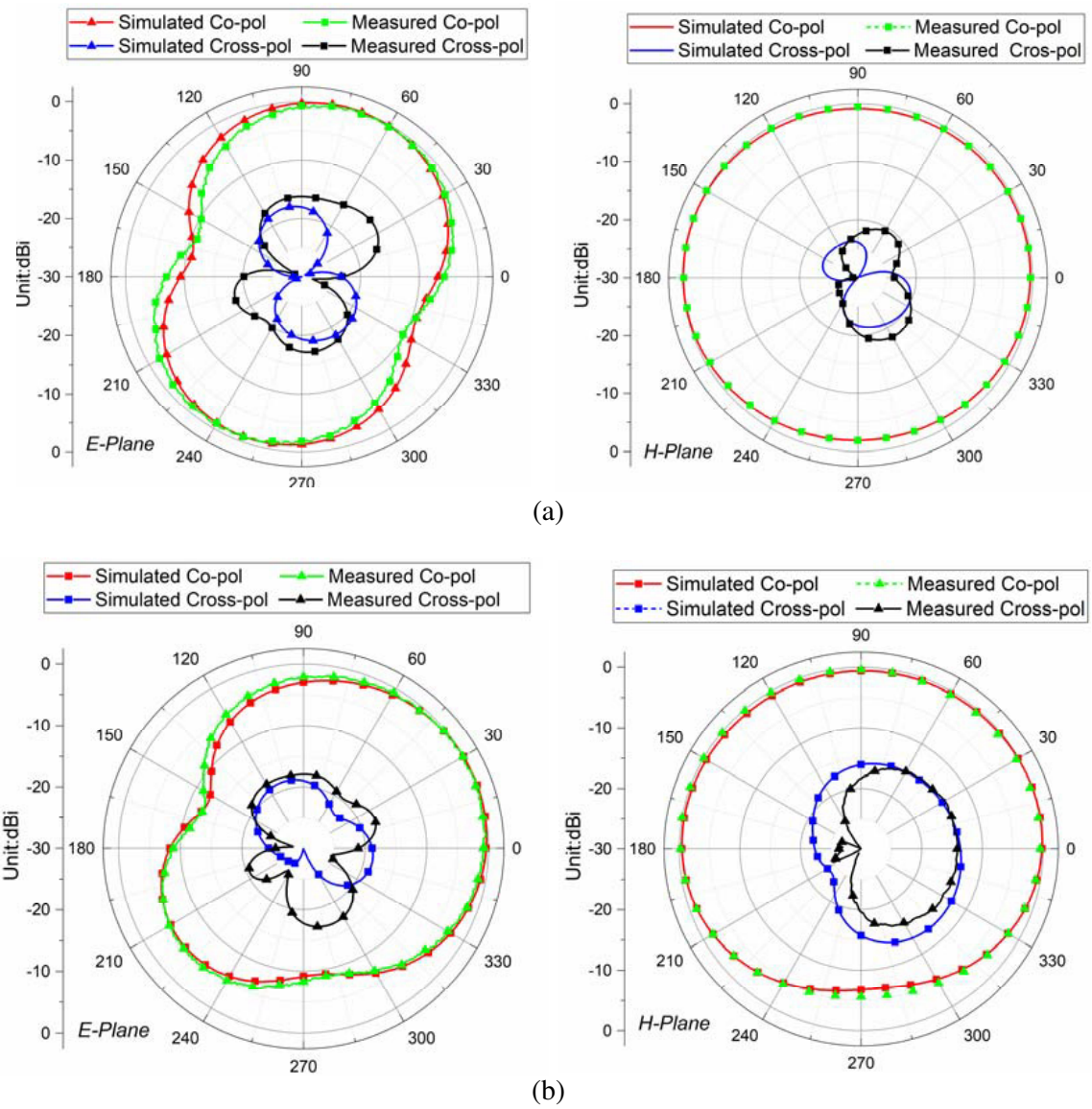

Figure 12. Simulated and experimental radiation patterns in both E- and H-planes at different frequencies. (a) 2.46 GHz, (b) 3.64 GHz.

The performance including size, peak gain and frequency band of the presented filtering antenna in this paper together with several other published filtering antennas reported in the references are summarized in Table 1 (where λ_g is the waveguide wavelength of these filtering antennas at the central frequency of the lowest operating frequency band). Compared with the antennas in [5, 10, 11], the proposed antenna is obviously compact. Besides, its higher band is controllable easily by adjusting the dimension of the T-shaped stub while leaving the lower band unaffected, which reduces the complexity of the design process.

4. CONCLUSION

The basic design principles have been explained to obtain a compact dual-band inverted-F filtering antenna with good band-edge selectivity for modern wireless communication systems. Firstly, a dual-band filter based on dual-mode resonators loading a T-shaped stub, which has three transmission zeros,

is designed and studied. Based on the transmission line theory, the resonant frequencies of the T-shaped stub loaded resonators are deduced. Then, a compact IFA also loading a T-shaped stub is designed and analyzed. The higher bands of both the filter and IFA are controllable easily by adjusting the dimensions of the T stub while the lower band is uninfluenced. For miniaturization, the last stage of the filter is modified. Ultimately, the miniaturized filter and IFA are integrated and optimized together. Compared with the traditional IFA, the filtering antenna obtains a flat gain response within the passband and has good band-edge selectivity.

REFERENCES

1. Fallahi, R., A. A. Kalteh, and M. G. Roozbahani, "A novel UWB elliptical slot antenna with band-notched characteristics," *Progress In Electromagnetics Research*, Vol. 82, 127–136, 2008.
2. Tang, M. C., H. Wang, T. Deng, and R. W. Ziolkowski, "Compact planar ultrawideband antennas with continuously tunable, independent band-notched filters," *IEEE Transactions on Antennas and Propagation*, Vol. 64, No. 8, 3292–3301, 2016.
3. Tao, J. and Q. Feng, "Compact UWB band-notch MIMO antenna with embedded antenna element for improved band notch filtering," *Progress In Electromagnetics Research C*, Vol. 67, 117–125, 2016.
4. Barbuto, M., F. Trotta, F. Bilotti, and A. Toscano, "Horn antennas with integrated notch filters," *IEEE Transactions on Antennas and Propagation*, Vol. 63, No. 2, 781–785, 2015.
5. Wu, W. J., Y. Z. Yin, S. L. Zuo, Z. Y. Zhang, and J. J. Xie, "A new compact filter-antenna for modern wireless communication systems," *IEEE Antennas and Wireless Propagation Letters*, Vol. 10, 1131–1134, 2011.
6. Wu, W., C. Wang, X. Wang, and Q. Liu, "Design of a compact fitler-antenna using DGS structure for modern wireless communication systems," *IEEE Int. Symp. Microwave, Antenna, Propag. EMC Technol. Wirel. Commun.*, 355–358, 2013.
7. Mansour, G., M. J. Lancaster, P. S. Hall, P. Gardner, and E. Nugoolcharoenlap, "Design of filtering microstrip antenna using filter synthesis approach," *Progress In Electromagnetics Research*, Vol. 145, 59–67, 2014.
8. Tang, M. C., Y. Chen, and R. W. Ziolkowski, "Experimentally validated, planar, wideband, electrically small, monopole filtennas based on capacitively loaded loop resonators," *IEEE Transactions on Antennas and Propagation*, Vol. 64, No. 8, 3353–3360, 2016.
9. Wu, W. J., Y. Z. Yin, J. J. Xie, X. S. Ren, and S. L. Zuo, "Low-cost microstrip filter antenna with a monopole-like radiation pattern for RF front end," *Microwave and Optical Technology Letters*, Vol. 54, No. 8, 1810–1814, 2012.
10. Yao, Y., Z. Tu, and Z. Gan, "A tri-band monopole filtering antenna using multimode resonators," *Microwave and Optical Technology Letters*, Vol. 59, No. 8, 1908–1913, 2017.
11. Hsieh, C. Y., C. H. Wu, and T. G. Ma, "A compact dual-band filtering patch antenna using step impedance resonators," *IEEE Antennas and Wireless Propagation Letters*, Vol. 14, 1056–1059, 2015.
12. Pozar, D. M., *Microwave Engineering*, 4th Edition, Wiley, New York, NY, USA, 2005.
13. Tsai, C., S. Y. Lee, and C. C. Tsai, "Performance of a planar filter using a 0° feed structure," *IEEE Transactions on Microwave Theory and Techniques*, Vol. 50, No. 10, 2362–2367, 2002.
14. Zhang, X. Y., J.-X. Chen, Q. Xue, and S.-M. Li, "Dual-band bandpass filters using stub-loaded resonators," *IEEE Microw. Wirel. Components Lett.*, Vol. 17, No. 8, 583–585, 2007.
15. Shi, J. and Q. Xue, "Balanced bandpass filters using center-loaded half-wavelength resonators," *IEEE Transactions on Microwave Theory and Techniques*, Vol. 58, No. 4, 970–977, 2010.
16. Hong, J.-S. and M. J. Lancaster, *Microstrip Filters for RF/Microwave Applications*, Wiley, New York, NY, USA, 2001.